https://doi.org/10.5194/egusphere-2025-2995
Preprint. Discussion started: 4 July 2025
© Author(s) 2025. CC BY 4.0 License.

Representing canopy structure dynamics within the LPJ-GUESS dynamic global vegetation model (revision 13221)

Jette Elena Stoebke[1,2,*], David Wårlind[1,*], Stefan Olin[1], Annemarie Eckes-Shephard[1], Bogdan Brzeziecki[3], Mikko Peltoniemi[4], and Thomas A. M. Pugh[1,5,6]

[1]Department of Physical Geography and Ecosystem Science, Lund University, 223 62 Lund, Sweden
[2]Institute of Marine Ecosystem- and Fishery Science, University of Hamburg, 22767 Hamburg, Germany
[3]Department of Silviculture, Institute of Forest Sciences, Warsaw University of Life Sciences, 02-776 Warszawa, Poland
[4]Natural Resources Institute Finland (Luke), 00790 Helsinki, Finland
[5]School of Geography, Earth and Environmental Sciences, University of Birmingham, Birmingham B15 2TT, UK
[6]Birmingham Institute of Forest Research, University of Birmingham, Birmingham B15 2TT, UK
[*]These authors contributed equally to this work and share first authorship

Correspondence: David Wårlind (david.warlind@nateko.lu.se)

Abstract. The competition for light is a fundamental determinant of the structure and composition of a forest. Large-scale forest models must balance real-world complexity with computational demand and poorly constrained parameters. The LPJ-GUESS dynamic global vegetation model has a strong track record of simulating forest composition and tree demography with a simple representation of forest canopies. The current approach, however, is limited in its ability to explore functional co-existence of trees within forest patches or to represent the full implications of forest management actions which create heterogeneous light conditions on the forest floor. The current representation of forest canopy in LPJ-GUESS is based on vertically overlapping crowns with no horizontal structure. Whilst computationally efficient, this approach does not allow for a realistic representation of forest floor light distribution following tree death or harvest.

Here we describe the implementation of a new scheme with spatially explicit canopies, where tree cohorts have a fixed position within a patch, enabling more realistic simulation of forest floor light conditions, especially following disturbances such as tree death or harvest. Additionally, we introduce a lower-complexity model version based on a perfect plasticity-like approximation.

To evaluate these developments, we conduct four assessments. First, we evaluate the model's performance against field observations of aboveground woody biomass, mortality, and productivity across diameter size classes. Second, we examine the ability to represent tree functional co-existence. Third, we explore how forest harvest influence the re-establishment of a woody understory. Lastly, we conduct two sensitivity tests.

Results show that the spatially explicit canopy schemes improve representation of forest size structure and dynamics across boreal, temperate, and tropical regions. It also enables representation of functional co-existence without the influence of large-scale disturbances and captures the interplay of forest gap dynamics with the establishment of a recruitment layer, capabilities not achievable with the standard canopy approach.

https://doi.org/10.5194/egusphere-2025-2995
Preprint. Discussion started: 4 July 2025
© Author(s) 2025. CC BY 4.0 License.

These advances significantly enhance the model's capacity to explore forest management effects and functional co-existence, and improve its alignment with observational data. The new canopy schemes offer a more robust foundation for modelling forest dynamics under historical, current, and future environmental conditions.

https://doi.org/10.5194/egusphere-2025-2995
Preprint. Discussion started: 4 July 2025
© Author(s) 2025. CC BY 4.0 License.

1 Introduction

Forest demography is the study of how tree populations change over time through processes such as recruitment, growth, and mortality. From these processes emerges a complex mosaic of individual trees of different size, age, and species. The emergent forest structure and composition then govern its capability to react to environmental changes, disturbances, and climate variability (Waring and Running, 2010). A correct forest structure and representation of demographic processes are therefore crucial for forecasting ecosystem services like carbon sequestration, biodiversity, and resilience to extreme events and disturbances (Brockerhoff et al., 2017; McDowell et al., 2020).

One of the primary drivers of forest dynamics is competition, whether for light, water, or nutrients, which shapes the structure and composition of vegetation within a forest. The vertical and horizontal distribution of trees within the forest canopy determines how photosynthetically active radiation (PAR) is partitioned, influencing the growth and productivity of different trees and other forest species. Taller trees typically absorb more light, overshadowing shorter trees in the understory, which affects their growth, survival, and succession (King, 1990; Niinemets and Kull, 1995). Not only does the vertical distribution of trees within the canopy play a crucial role, but spatial interactions in general. As neighbouring trees compete for resources, their spatial arrangement determines their individual success, as well as the overall structure and function of the forest (Pacala and Deutschman, 1995; Kunstler et al., 2012). Physical arrangements and interactions result in the establishment of spatial heterogeneity, supporting the creation of canopy gaps, which allow light to reach various forest layers, facilitating species co-existence, succession, and the promotion of biodiversity by generating diverse micro-environments (Brokaw and Busing, 2000). Beyond that, disturbances, ranging from individual tree mortality to large stand-replacing events, further shape forest structure and composition (Hardiman et al., 2013). The dynamic interplay between light availability, stand structure, and disturbance regimes drives ecological processes such as species interactions and forest succession. Such processes, in turn, influence ecosystem resilience, helping forests recover from disturbances and maintain their ecological function.

To understand this complex interplay of forest dynamics, simulating forest demography is a critical tool to advance our understanding of forest ecology (Lavorel and Garnier, 2002). Through the simulation of vegetation demography, we can gain insights into plant population interactions, ecosystem health, and resilience, as well as better predict environmental responses and inform sustainable forest management strategies (Sitch et al., 2008). In recent years, various approaches have been developed to model forest dynamics, striving to balance model fidelity with its complexity (Fisher et al., 2018). Vegetation demographic models (VDMs) are powerful tools for generating ecological forecasts, as they simulate the complex interactions between plants, climate, and both biotic and abiotic factors. These models typically incorporate key processes such as photosynthesis, respiration, as well as carbon, nutrient, and water cycling, all of which are essential for capturing the complex functioning of ecosystems (Fisher et al., 2018). By resolving demographic processes, VDMs can represent how plant populations respond to internal dynamics and external drivers, such as climate change, land-use change, management or natural disturbances. One such model, LPJ-GUESS, has represented forest demography for over 25 years. LPJ-GUESS uniquely combines an individual- and patch-based representation of vegetation dynamics with ecosystem biogeochemical cycling, making it well-suited for simulating forest structure, species composition, and demographic processes (Smith et al., 2001, 2014).

https://doi.org/10.5194/egusphere-2025-2995
Preprint. Discussion started: 4 July 2025
© Author(s) 2025. CC BY 4.0 License.

Over the years, LPJ-GUESS has proven to be highly capable of modelling forest ecosystem processes. The representation of vegetation composition and structure is achieved by grouping tree individuals based on their plant functional types (PFTs) and age classes into cohorts, which represent groups of trees with similar ecological characteristics. These cohorts compete for essential resources such as light, water, nutrients, and space within a modelled area (patch). By simulating the competition between cohorts of different PFTs and age classes, LPJ-GUESS captures changes in forest structure and composition over time, especially in response to stand-replacing disturbances (Hickler et al., 2012; Smith et al., 2014; Pugh et al., 2024). Such simulations reflect natural forest succession, where cohorts of fast-growing, shade-intolerant and early successional PFTs occupy open areas, rapidly generating shade that suppresses their own seedlings. As the forest matures, the environment becomes more conducive to the establishment of shade-tolerant, late successional PFT cohorts. LPJ-GUESS not only represents vegetation composition and structure, but also simulates the effects of disturbances on forests, including changes to their age structure and productivity. As an example, LPJ-GUESS simulates how changes in disturbance regimes, such as shifts in the frequency of stand replacing events, can significantly influence the forest carbon sink, either increasing or decreasing it depending on disturbance return times and forest type (Pugh et al., 2019b). Also, the simulation of fire regimes and their impact on forest demography provide valuable insights into how changing fire frequencies influence forest composition and structure (D'Onofrio et al., 2020). Furthermore, LPJ-GUESS incorporates nutrient limitations, which are critical in shaping forest composition and structure. When simulating boreal forests, for instance, alleviating nutrient limitations on productivity would lead to forest densification in a warmer future climate (Wårlind et al., 2014). All in all, these capabilities make LPJ-GUESS a versatile tool for simulating forest dynamics in response to a wide range of ecological and environmental factors. While LPJ-GUESS has proven successful in modelling dynamic forest responses thanks to representing demography the increasing availability of observational data has revealed limitations in the model pertaining to capturing finer-scale processes (Pugh et al., 2019c; Dietze et al., 2018; Van der Plas et al., 2018). For instance, the model relies on stand-replacing disturbances as proxies for all types of disturbances, an oversimplification that leads to the under-representation of vertical forest structure shaped by smaller-scale disturbances, which are more common in reality. As a consequence, it struggles to accurately represent tree size distribution and species composition, when assessed at small scale. For example, LPJ-GUESS tends to simulate a persistent dominance of late-successional PFTs in old-growth forests, which may overlook the ongoing compositional changes and structural complexity present in many natural forests. While such dominance has been documented in certain systems (Brzeziecki et al., 2020), numerous old-growth forests continue to exhibit dynamic and diverse community structures over time (Waterman et al., 2020).

For instance, the model relies on stand-replacing disturbances as proxies for all types of disturbances, an oversimplification that leads to the under-representation of vertical forest structure shaped by smaller-scale disturbances, which are more common in reality. LPJ-GUESS also has difficulties in simulating regeneration patterns after natural mortality or harvest events, where pioneer PFTs should rapidly colonise newly created gaps. Moreover, the model tends to simulate a persistent dominance of late-successional PFTs in old-growth forests, which may overlook the ongoing compositional changes and structural complexity present in many natural forests. While such dominance has been documented in certain systems (Brzeziecki et al., 2020), numerous old-growth forests continue to exhibit dynamic and diverse community structures over time (Waterman et al., 2020). Incorporating horizontal variability within forest ecosystems is another crucial consideration. For example, LPJ-GUESS has

https://doi.org/10.5194/egusphere-2025-2995
Preprint. Discussion started: 4 July 2025
© Author(s) 2025. CC BY 4.0 License.

difficulties in simulating regeneration patterns both after natural mortality and harvest events, where pioneer PFTs should rapidly colonise newly created gaps. Pacala and Deutschman (1995) demonstrated that mean-field models, i.e. models which often ignore horizontal heterogeneity within a patch, can underestimate basal area by as much as 50% compared to models that account for spatial variability, underscoring the importance of integrating horizontal elements into forest demographic simulations.

The mentioned shortcomings point to the need for improvements, particularly in the model's canopy structure representations which is central to simulating small-scale forest dynamics. Currently, LPJ-GUESS distributes tree crown area evenly across the patch, resulting in a uniform light distribution, even when the total crown area is smaller than the patch area. This uniformity prevents the formation of light gaps, hampering regeneration and species co-existence. To address this issue, we have developed a new light transmission scheme called the "spatially-explicit canopy" (SEC). This novel scheme aims to provide a more accurate representation of the horizontal canopy structure, particularly in the absence of large disturbances, as well as to enhance species co-existence and allow for the simulation of re-establishment in relatively small canopy gaps following tree mortality events.

In this paper, we present a detailed description of the spatially-explicit canopy scheme, SEC, and evaluate its performance in several key areas. We (1) evaluate its ability to capture stand structure and dynamics using data from forests around the world, (2) assess its improved representation of functional co-existence of tree sizes and species compared to the standard model, (3) examine how sensitive the simulated re-establishment is to different harvest intensities, as a proxy for gap size, and (4) test the model's responsiveness to key parameters, such as wood density, establishment rates, and mortality.

2 Methods

2.1 Model description

Historically, LPJ-GUESS (Smith et al., 2001, 2014; Sitch et al., 2003) employed a "vertically overlapping crowns" approach to represent canopy structure (Fig. 1a), which was referred to as LPJ in this context. In the LPJ model, horizontal spatial structure within a patch was not considered for light absorption. Instead, the model focused solely on vertical structure based on the bole and total height of each tree cohort. The actual crown area was not directly accounted for, as the leaf area of each cohort was conceptually distributed uniformly both horizontally across the entire patch and vertically through the canopy.

The fraction of incoming PAR ($fPAR$) absorbed by each cohort was calculated using the Lambert-Beer law (Prentice et al., 1993; Smith et al., 2001), which assumed that cohorts shaded themselves and all cohorts beneath them.

$$fPAR(z) = 1 - e^{-kLAI(z)} \tag{1}$$

where $fPAR(z)$ was $fPAR$ at canopy depth z (m), k was the light extinction coefficient, and $LAI(z)$ was the summed leaf-area index (LAI; $\mathrm{m}^2\,\mathrm{m}^{-2}$) of leaves from all cohorts above canopy depth z. For canopy sections with more than one cohort, $fPAR$ was distributed among the cohorts based on each cohort's LAI fraction in that section, assuming that all cohorts shared the same extinction coefficient (k). For the canopy illustrated in Fig. 1a, this resulted in seven distinct vertical sections

https://doi.org/10.5194/egusphere-2025-2995
Preprint. Discussion started: 4 July 2025
© Author(s) 2025. CC BY 4.0 License.

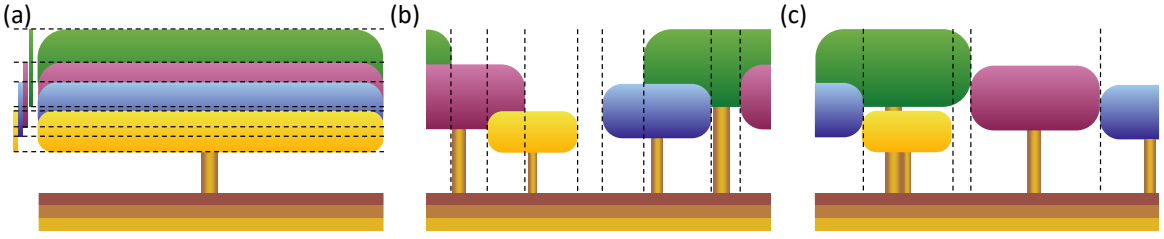

Figure 1. Canopy structure representation of four tree cohorts in a single LPJ-GUESS patch. (a) Standard LPJ-GUESS (LPJ) – In this model, the canopy lacks a heterogeneous horizontal structure. The leaf area is evenly distributed across the entire patch area, and the canopy structure is determined solely by the tree and bole height of each cohort. In this example the canopy has a sole horizontal section with seven distinct vertical sections in which light absorption needs to be calculated. The bars on the left visualise the depth of each cohort's canopy. (b) Spatially-explicit canopy (SEC) – Cohorts have fixed positions within the patch. When a tree dies, it creates a gap in the canopy. This gap persists over time, allowing new tree cohorts to establish and grow under full light conditions. This example has eight distinct horizontal sections, with their individual light conditions vertically determined in a similar manner as for (a). (c) Perfect plasticity-like approximation (PPL) – Cohorts are organised by tree height, filling the patch area perfectly. The tallest tree cohorts fill the patch until the cumulative crown area equals or exceeds the patch area. Once the patch is filled, an understory layer is formed with the next shorter tree cohort. This example has five distinct horizontal sections.

that needed to be calculated to determine each cohort's $fPAR$. The remaining $fPAR$ ($fPAR_{herb,top}$) become available on the forest floor for absorption by the herbaceous understory. The total forest floor PAR over the year (PAR_{est}; $\mathrm{J\,m^{-2}\,day^{-1}}$) determined whether the light conditions were sufficient for a specific PFT to establish and also influenced the biomass of newly established saplings. The minimum light condition ($PAR_{est,min}$; $\mathrm{J\,m^{-2}\,day^{-1}}$) required for fast-growing, shade-intolerant pioneer PFTs was higher than that for slow-growing, shade-tolerant PFTs. In the LPJ approach, the uniform distribution of each cohort's leaf area across the entire patch ensured that there were no canopy gaps that would allow full light to reach the forest floor, as long as a tree cohort was present. Typically, consistent shading provided an advantage to slow-growing, shade-tolerant PFTs, as the forest floor remained constantly shaded. Instead of actual canopy gaps, the LPJ model simulated canopy gap dynamics by using a large set of replicate patches. Each patch faced a patch-destroying disturbance with a probability corresponding to an average return interval of 100 years (Smith et al., 2014; Pugh et al., 2019a). In this study, we examind the effect of this patch-destroying disturbance by having it turned on (LPD) and off (LPJ). Another issue with uniformly distributed leaf area across the patch was that in a patch with a single tree cohort, where its total crown area (CA_i; $\mathrm{m^2}$) only covered a fraction of the patch, the $fPAR$ was overestimated, according to eqn 1, compared to if the leaves only covered the actual crown area. This occurred because the leaves were spread over a larger area, resulting in less self-shading compared to what would occur with a more realistic crown area. Consequently, this could lead to an unrealistically low tree density (under-crowding). In highly productive sites, a single large cohort with high LAI could shade all shorter cohorts, potentially leading to their death. This occurred even though the taller cohort's CA_i might have covered only a fraction of the patch. Conversely, over-crowding could occur because the CA_i did not limit tree density in a patch unless CA_i of an individual cohort exceeded its maximum

https://doi.org/10.5194/egusphere-2025-2995
Preprint. Discussion started: 4 July 2025
© Author(s) 2025. CC BY 4.0 License.

available crown area ($CA_{max,i}$; m^2), which was the entire patch area in LPJ. In such cases, the individual cohort underwent self-thinning by increasing its probability of mortality ($mort_{self}$).

$$mort_{self} = \frac{CA_i - CA_{max,i}}{CA_i} \tag{2}$$

The SEC canopy scheme was introduced to overcome the limitations associated with the absence of horizontal spatial structure. In SEC (Fig. 1b), cohorts were assigned fixed positions within the patch, enabling gaps created by tree mortality to persist over time. These gaps provided optimal light conditions at the forest floor, promoting the establishment of shade-intolerant PFTs. Over time, the size of the gap decreased as overstory cohorts grew, occupying more space as their crown area increased. Each cohort's position was defined in a two-dimensional space (Θ, z), where Θ ($\Theta \in [0, 2\pi]$) represented its placement on a ring. This method eliminated border issues, as each cohort seamlessly continued in space (see green and purple cohorts in Fig. 1b). The calculation of $fPAR$ for each cohort followed a similar method to LPJ, using Eqn. 1. First, unique vertical sections were identified (eight in Fig. 1b). The light absorption in each section was then calculated using the same approach as employed in LPJ. Unlike LPJ, the SEC approach then considered the variation in forest floor light conditions across the different sections. This made it possible for the leaf area of the herbaceous understory to be dynamically adjusted for each horizontal section to optimise total light absorption. Since the minimum PAR requirement for establishment varied among PFTs, the fraction of the patch where each PFT could be established also differed. The forest floor was divided into a fixed number of horizontal sections (N_{ff}; set to 100 in this study), with annual PAR calculated for each section. Consequently, only a fraction of these sections (f_{est}; Fig. 2) had light conditions that met $PAR_{est,min}$ for a specific PFT. If a new cohort could not be established across the entire patch area, the number of saplings in the new cohort was reduced by f_{est}. Additionally, $CA_{max,i}$ was updated, as self-thinning occurred when CA_i exceeded f_{est} plus the crown area of an individual tree of the cohort. The biomass of newly established saplings was also adjusted by $f_{est,bm}$ (Eqn 3; Fig. 2) to account for the mean PAR_{est} relative to the maximum PAR ($PAR_{est,max}$; $\mathrm{J\,m^{-2}\,day^{-1}}$) in the forest floor sections that met the establishment requirements ($N_{ff,est}$)

$$f_{est,bm} = \frac{1}{N_{ff,est}} \sum_{i=1}^{N_{ff}} \begin{cases} 0 & PAR_{est,i} \leq PAR_{est,min} \\ \frac{PAR_{est,i}}{PAR_{est,max}} & PAR_{est,i} > PAR_{est,min} \end{cases} \tag{3}$$

Each new PFT cohort's position was randomly selected from a weighted probability distribution based on the light conditions of each forest floor section that exceeded $PAR_{est,min}$.

For comparison, we also introduced a perfect plasticity-like (PPL) approximation canopy scheme in LPJ-GUESS, loosely based on the work of Purves et al. (2008) and Fisher et al. (2010, 2018). In PPL, tree cohorts were organised according to height and were arranged to perfectly fill the patch area. The tallest cohorts were assigned to the patch until their cumulative crown area equalled or exceeded the patch area. Once the patch was filled, an understory layer was created with the next tallest tree cohorts. If a cohort's crown area could not fully fit within a single canopy layer, it was distributed across multiple layers (see blue cohort in Fig. 1c). Horizontal sections and light absorption within them were determined as per the SEC, which resulted in the creation of five distinct vertical light conditions for the example in Fig. 1c. The herbaceous layer and light conditions

https://doi.org/10.5194/egusphere-2025-2995
Preprint. Discussion started: 4 July 2025
© Author(s) 2025. CC BY 4.0 License.

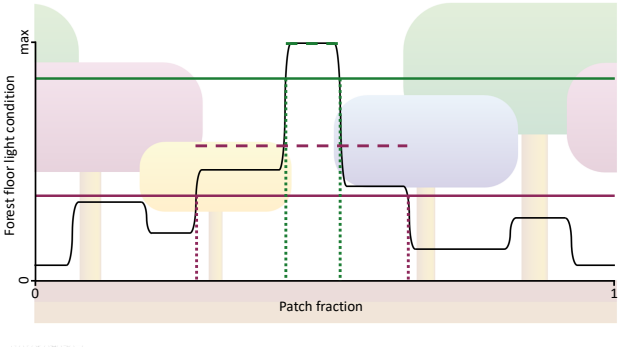

Figure 2. A visualisation of $f_{est,bm}$ and f_{est} for new establishment using SEC (Fig. 1b). The visualisation includes the establishment of two PFTs: a shade-intolerant pioneer PFT (green lines) and a slow-growing, shade-tolerant PFT (purple lines). The range between dotted lines represents f_{est}, while the dashed lines indicate the mean $PAR_{est,i}$ for the f_{est} ranges, and the solid lines show $PAR_{est,min}$. The value of $f_{est,bm}$ is calculated as the ratio between the mean $PAR_{est,i}$ to $PAR_{est,max}$ described in eqn 3.

for establishment were modelled similarly to the SEC approach. In the standard perfect plasticity approximation (PPA) model (Fisher et al., 2018), each understory canopy layer received the average light that penetrated through the layer above it. As a result, the position and height of cohorts within these layers became redundant, except for their allocation to specific layers. In contrast, our approach assigned cohorts a specific vertical position based on their height, enabling understory cohorts to intersect with the canopy layer above them if their height exceeded the bole height of the cohort above (see blue and green cohorts in Fig. 1c). Both PPA and PPL shared similar challenges to LPJ when it came to gap dynamics. If the total crown area of all cohorts exceeded the patch area, no gaps formed within the canopy. To address this, the PPA scheme (Fisher et al., 2018) introduced a gap fraction (η) that represented small gaps between trees within a cohort (Weng et al., 2015; Fisher et al., 2018). This feature allowed more light to penetrate the canopy layers, improving light conditions for the understory and resulting in more realistic understory behaviour. However, our PPL representation did not incorporate this gap fraction, so that gaps only occurred when the total crown area of all cohorts was less than the patch area. Instead, we focused on structural features, such as tree and bole height, crown area, and cohorts' light interactions, as described earlier, as well as distinct forest floor light conditions for establishment. We considered these aspects to be more relevant to our study. Additionally, both PPA and PPL methods for organising the canopy horizontal structure led to dynamic promotion and demotion of cohorts between layers, depending on growth and mortality.

One limitation shared by all of the schemes was that tree individuals within a cohort did not interact with one another in terms of shading. They were positioned in perfect alignment, with no overlap in their crowns. As a result, the total crown area (CA_i) for each cohort increased linearly as the identical trees in the cohort grew. Additionally, none of the schemes accounted for the angle of the sun (e.g. see Sato et al. (2007)), assuming instead that all solar radiation came directly from the zenith. It was also worth noting that individual calibrations for each canopy scheme had not been performed. Since LPD was the standard canopy scheme for LPJ-GUESS, it had undergone extensive calibration over the years.

https://doi.org/10.5194/egusphere-2025-2995
Preprint. Discussion started: 4 July 2025
© Author(s) 2025. CC BY 4.0 License.

Table 1. Description of the plant function types included in the study.

PFT	Description	Shade tolerance	$PAR_{est,min}$	k_{reprod}	$greff_{min}$
BNE	Boreal needleleaved evergreen tree	Shade-tolerant	350000	200	0.03
BINE	Boreal needleleaved evergreen tree	Shade-intolerant	2500000	800	0.09
BNS	Boreal needleleaved summergreen tree	Shade-intolerant	2500000	800	0.09
TeNE	Temperate needleleaved evergreen tree	Shade-intolerant	2500000	800	0.09
IBS	Broadleaved summergreen tree	Shade-intolerant	2500000	800	0.135
TeBS	Temperate broadleaved summergreen tree	Shade-tolerant	350000	200	0.03
TeBE	Temperate broadleaved evergreen tree	Shade-tolerant	350000	200	0.03
TrBE	Tropical broadleaved evergreen tree	Shade-tolerant	350000	200	0.03
TrIBE	Tropical broadleaved evergreen tree	Shade-intolerant	2500000	800	0.09
C3G	Cool (C3) grass	-	1000000	-	-
C4G	Warm (C4) grass	-	1000000	-	-

2.2 Model simulations

To validate the new canopy structure schemes, we perform model simulations using all four vegetation canopy structure schemes: LPJ, LPD, PPL, and the SEC scheme. The model simulations are driven by the CRUNCEP global reanalysis climate dataset version 7 (Viovy, 2016), using a 30-year de-trended historical climatology from 1971 to 2000 to establish an equilibrium vegetation condition over a 500-year period. During this spin-up phase, a stochastic, generic patch-destroying disturbance with a mean return interval of 100 years is introduced. After 500 years, a disturbance event resets the vegetation to bare ground, initiating a regrowth phase that lasts for an additional 1000 years under the same de-trended climate forcing. During this regrowth phase, no further disturbances are introduced, except in the LPD simulations, where disturbances continue with a 100-year mean return interval. All simulations use 100 replicate patches, with the exception of a sensitivity test that explores the impact of varying the number of patches. Fire is disabled for all simulations. The model is set up with 11 PFTs as described in Table 1.

2.3 Model evaluations

The model evaluation for stand structure and dynamics primarily relies on observations of aboveground woody biomass (AGB; $\mathrm{tC\,ha^{-1}\,cm^{-1}}$ DBH), aboveground woody mortality (AWM; $\mathrm{tC\,ha^{-1}\,yr^{-1}\,cm^{-1}}$ DBH), and aboveground woody productivity (AWP; $\mathrm{tC\,ha^{-1}\,yr^{-1}\,cm^{-1}}$ DBH) collected from 25 large forest plots, as presented by Piponiot et al. (2022). For model comparison reasons the data was processed to tC $\mathrm{ha^{-1}}$ $\mathrm{yr^{-1}}$ $\mathrm{cm^{-1}}$ DBH. AGB, AWP and AWM are provided across different diameter at breast height (DBH) size classes. For AGB, we standardised the observations into 16 DBH size classes: <1, <5, <10, <15, <20, <30, <40, <50, <60, <70, <80, <90, <100, <150, <200, and >200 cm. For AWM and AWP, the data were

https://doi.org/10.5194/egusphere-2025-2995
Preprint. Discussion started: 4 July 2025
© Author(s) 2025. CC BY 4.0 License.

already standardised into 9 DBH size classes: <5, <10, <20, <30, <40, <50, <100, <200, and <500 cm. We excluded the smallest and largest size classes (<1 and >200 cm) for AGB as well as the largest size class (<500) for AWP and AWM.

The forest plots: SERC, MBW, and Palamnui were excluded from the analysis due to low growth biases detected during initial LPJ-GUESS simulations. Since this study aims to assess the impact of the new canopy structure representation rather than basic growth processes, these sites were not suitable for our tests. Additionally, the San Lorenzo site was excluded because its coordinates, when converted to the climate forcing resolution, correspond to those of Barro Colorado Island. Additionally, the Barro Colorado Island entry was updated to match the data provided by Legendre and Condit (2019). In reviewing the dataset, it should be noted that some data from Piponiot et al. (2022) were gap-filled where differences between observed and expected values occurred. Additionally, several study sites have been subject to disturbance events of both natural and human origin. Table 2 offers a summary of all study sites and documented disturbances, although quantitative details remain limited for most events (Piponiot et al., 2022). In addition to the existing study sites, we incorporated AGB data from old-growth forests in five permanent monitoring plots within Białowieza National Park (Poland) by Brzeziecki et al. (2016) as well as data from 57 unmanaged sites across southern and central Finland by Peltoniemi and Mäkipää (2011). To ensure consistency across datasets, we interpolated the original DBH size classes from these sources to match the 16 DBH size classes used in the data compiled by Piponiot et al. (2022). This resulted in a total of 23 study sites distributed across five continents, representing three major forest temperature regions: 14 tropical, 5 temperate, and 4 boreal sites (Table 2). The sites are located in both old-growth and mature secondary forests.

Our evaluation of the four vegetation schemes will focus on several key metrics. First, we will assess the accuracy of each scheme in replicating AGB, AWM, and AWP as a function of DBH size classes, comparing the results with observational data. Second, we will examine the emergence of self-thinning patterns, mortality fluxes and rates, and the dynamics of functional co-existence within each scheme. Third, we will analyse the re-establishment process following harvesting events across the different schemes. Fourth, we will conduct two sensitivity tests: the first will assess how variations in wood density, establishment, and mortality rates affect functional co-existence, and the second will investigate how the RMSE of AGB, AWM, and AWP, compared to observations, converges as the number of replicate patches increases.

The first two metrics will be evaluated based on the basic model simulations across all 23 study sites. The analysis of the re-establishment process, as well as the sensitivity tests, will be conducted using modifications to the basic simulations. For the third analysis (re-establishment processes following a harvesting event), the 1000-year regrowth phase will be replaced with a harvesting event that occurs 80 years after the initial patch-destroying disturbance. Since re-establishment varies with harvest intensity, harvest events of the dominant cohorts will be induced at different intensities: 0% as a control, 10%, 20%, 30%, 40%, 50%, 60% and 70%. Post-harvest biomass in the recruiting layer will be compared with the total biomass at 10, 30, and 60 years after the event. LPD simulations will be excluded from this analysis to ensure that patch-destroying disturbances do not affect the outcome. This analysis will be carried out exclusively at the BCI site. The functional co-existence sensitivity tests involve pushing three key parameters in LPJ-GUESS to their extremes to examine the potential for co-existence between shade-intolerant and tolerant PFTs over time. First, we will test the effect of wood density by doubling the wood density of shade-tolerant PFTs, allowing shade-intolerant PFTs to grow taller faster than shade-tolerant PFTs. Secondly, we will make the

https://doi.org/10.5194/egusphere-2025-2995
Preprint. Discussion started: 4 July 2025
© Author(s) 2025. CC BY 4.0 License.

Table 2. Overview of the study sites.

Study site	Area (ha)	Region	Longitude	Latitude	Information
Amacayacu	25.0	Trop	-70.27	-3.81	Partly flooded[1]
Barro Colorado Island	50.0	Trop	-79.85	9.15	Small-scale disturbance, ENSO-driven droughts[2]
Białowieza	15.4	Temp	23.75	52.75	No major disturbance[3]
Changbaishan	25.0	Boreal	128.08	42.38	Wind, insect outbreaks[4]
Cocoli	4.0	Trop	-79.62	9.99	El Nino[5]
Danum Valley	50.0	Trop	117.69	5.1	Drought (1997-1998)[6]
Edoro	20.0	Trop	28.52	1.56	No major disturbance
Finland	*	Boreal	23.25	62.25	No major disturbance[7]
Fushan	25.0	Temp	121.56	24.76	Typhoon[8]
Gutianshan	24.0	Temp	118.12	29.25	No major disturbance
Korup	50.0	Trop	8.85	5.07	Wind throw, lightning, diseases, fires[9]
Lambir	52.0	Trop	114.02	4.19	Drought (1998)[10]
Laupahoehoe	4.0	Trop	-155.29	19.93	Surface water flow[11]
Lenda	20.0	Trop	28.65	1.32	No major disturbance
Luquillo	16.0	Trop	-65.82	18.33	Hurricanes, landslides, droughts[12]
Mudumalai	50.0	Trop	76.53	11.6	Winter monsoon, damage through mammals[13]
Pasoh	50.0	Trop	102.31	2.98	Pig disturbances[14]
SCBI	25.6	Temp	-78.15	38.89	Deer browsing[15]
Sinharaja	25.0	Trop	80.4	6.4	Small-scale disturbance, selective logging[16]
Wabikon	25.2	Boreal	-88.79	45.55	No major disturbance
Wanang	50.0	Trop	145.27	-5.25	Undercutting of trees[17]
Wind River	27.2	Boreal	-121.96	45.82	Fire (before forest establishment)[18]
Zofin	25.0	Temp	14.71	48.66	Windstorms[5]

* 57 unmanaged sites across southern and central Finland (Peltoniemi and Mäkipää, 2011).

References: [1]López-Quintero et al. 2012, [2]Koven et al. 2020, [3]Brzeziecki et al. 2020, [4]Zhang et al. 2023, [5]Piponiot et al. 2022, [6]Douglas and Douglas 2022, [7]Peltoniemi and Mäkipää 2011 [8]Lin et al. 2011,[9]Egbe et al. 2012, [10]Potts 2003, [11]Michael and Hotchkiss 2009, [12]Zimmerman et al. 2021, [13]Sukumar et al. 2004, [14]Peters 2001, [15]Holm et al. 2013, [16]Alwis et al. 2016, [17]Vincent et al. 2015, [18]Shaw et al. 2004

establishment of new saplings more uniform across all PFTs by increasing the background establishment factor ($k_{bgestab} = 0.1$) and reducing the PFT-specific reproduction constant (k_{reprod}) by a factor of ten (Eqn 21 in Smith et al. 2001). This change will provide less dominant PFTs with a greater opportunity to establish. Finally, the growth efficiency mortality threshold (Eqn 31 in Smith et al. 2001), which determines the minimum growth efficiency ($gref f_{min}$; $\mathrm{kgC\,m^{-2}\,leaf\,yr^{-1}}$) below which mortality occurs, will be lowered for shade-intolerant PFTs to match that of shade-tolerant PFTs. Lastly, we will evaluate the impact of the number of replicate patches on the RMSE of AGB, AWM, and AWP, relative to observations. For this test, all sites except

https://doi.org/10.5194/egusphere-2025-2995
Preprint. Discussion started: 4 July 2025
© Author(s) 2025. CC BY 4.0 License.

BCI, BIA, and Finland will be rerun with varying numbers of replicate patches (1, 2, 5, 10, 15, 20, 30, 50, and 100) over the full simulation period.

2.4 Analysis framework

The model's performance is evaluated against observational data using the final simulation year. Both the model output and observation data are classified into the same DBH size classes: 16 classes for AGB and 9 classes for AWM and AWP. To ensure comparability across DBH distributions, both datasets are standardised to values per unit cm of DBH. For further analysis, AWM is normalised by AGB to provide a comparison of the aboveground woody mortality rate, rather than the flux itself. This approach is applied to both the observational and model data. All study sites are evaluated individually and as regional averages based on temperature. Białowieza and Finland are excluded from the analysis of AWM and AWP due to missing data. Independently of the observation data, the model's mortality fluxes are further analysed in order to understand the changing drivers of mortality. This analysis is performed for both LPJ and SEC, considering the total of above- and below-ground mortality instead of AWM. The fluxes include age mortality, self-thinning mortality, growth efficiency mortality, and other mortality. Self-thinning and growth efficiency mortality are grouped into a single class. The analysis does not consider DBH size classes, as fluxes are summed across all size classes and evaluated over the entire 1000-year regrowth period. Mortality rates are computed by dividing fluxes by the total biomass.

Self-thinning dynamics are assessed by examining the relationship between the number of trees (N; ha^{-1}) and the square root of their average quadratic mean diameter (Dg; cm), following Reineke (1933) and Bellassen et al. (2010), during the stand regrowth (years 10 to 100) and equilibrium (years 600 to 1000) phase

$$ln\,(N) = c_0 + c_1 ln\,(Dg) \tag{4}$$

where c_0 is the intercept and c_1 is the slope.

To analyse functional co-existence, we examine biomass over the entire time series, averaging across all sites, and with PFTs categorised into three groups: shade-tolerant, shade-intolerant, and grass. This grouping allows for a meaningful comparison of study sites with varying PFT compositions. The re-establishment test defines the recruitment layer as cohorts with a DBH smaller than 15 cm. The biomass of the recruitment layer is divided by total biomass to determine the fraction of biomass in the recruitment layer. The impact of varying simulated patch numbers is evaluated by computing the normalised distribution of AGB, AWM, and AWP across DBH classes, and then calculating the RMSE relative to observations. This test does not focus on the absolute values but on the speed at which different canopy structure schemes converge to estimate the optimal number of patches required for each scheme.

https://doi.org/10.5194/egusphere-2025-2995
Preprint. Discussion started: 4 July 2025
© Author(s) 2025. CC BY 4.0 License.

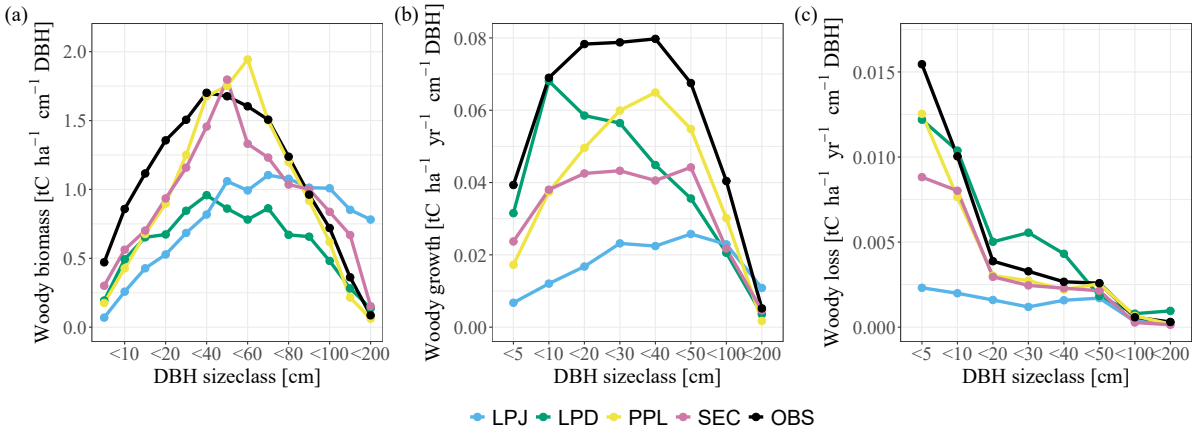

Figure 3. Comparisons of (a) woody biomass, (b) aboveground woody productivity and (c) aboveground woody mortality as a function of DBH size class as an average over all study sites.

3 Results

3.1 Stand structure and dynamics evaluation

When comparing the biomass distribution across size classes (Fig. 3a) for the final simulation year against the combined observational data from all biomes, LPJ generally captures the biomass distributions of large size classes in temperate and boreal regions (Fig. A1), but tends to underestimate biomass in smaller size classes. The overall overestimation is primarily driven by excessive biomass in large size classes at tropical sites. Conversely, LPD exhibits a notable leftward shift in the distribution towards smaller size classes. This shift is a result of the recurring patch-destroying disturbances that reset the patches to bare ground, increasing the occurrence of small size class trees. Consequently, LPD significantly underestimates total biomass compared to the observations. Similar to LPD, PPL and SEC simulate a greater biomass fraction in smaller trees. Their more detailed canopy structure allows them to better align overall biomass with the observations, particularly at the tropical study sites. LPJ and SEC have the highest total mean biomass across the sites of the schemes with 196 and 161 tC ha^{-1}, respectively. This is caused by having the highest biomass in the large DBH size classes. PPL has a total mean biomass of 133 tC ha^{-1} and LPD the lowest with 113 tC ha^{-1}. The reason for such low overall biomass for LPD (Fig 3a) lies again in the recurring patch-destroying disturbances. The biases in woody biomass-size distributions are ultimately caused by the interaction between growth and mortality rates. When comparing the simulated growth rates to observations over all sites, it becomes evident that all canopy schemes underestimate the AWP flux (Fig. 3b). This general underestimation is likely a result of other model biases not related to the canopy scheme, e.g. GPP or allocation of C to wood, which is beyond the scope of this work to address. What is more important for this study is the shape of the growth and mortality per DBH size classes, as compared to the observations. In this regard, LPJ significantly underestimates the AWP flux across all size classes, except for the largest trees. Conversely, LPD exhibits a bias towards smaller size classes, consistent with its woody biomass bias. PPL

https://doi.org/10.5194/egusphere-2025-2995
Preprint. Discussion started: 4 July 2025
© Author(s) 2025. CC BY 4.0 License.

and SEC simulate an AWP flux distribution across size classes that more closely align with observations, although the absolute values remain lower, with PPL being closest to observed values. When analysing individual regions, all canopy schemes tend to underestimate the AWP flux in tropical and temperate study sites (Fig. A2). In boreal study sites, AWP flux for smaller size classes (up to <30) is overestimated by all canopy schemes except for LPJ, whereas larger size classes are consistently underestimated. Overall, LPJ allocates an overly large fraction of the AWP flux to large trees, while LPD disproportionately assigns a larger fraction of the AWP flux to smaller trees. In contrast, PPL and SEC successfully capture the broad patterns of AWP flux distribution. Similar to the fluxes of AGB and AWP, LPJ tends to underestimate the AWM fluxes for smaller size classes (Fig. 3c) and cannot capture the AWM flux pattern for any of the tropical, temperate, and boreal study regions (Fig. A3). LPD, PPL, and SEC have the same issue in the boreal study sites. However, they exhibit a better agreement with observed patterns in tropical and temperate regions.

All canopy models exhibit emergent self-thinning behaviour when averaged across all sites during the initial regrowth phase, the first 100 years of stand development (coloured circles in Fig. 4). In the LPJ model, tree numbers decline clearly as mean stem diameter increases throughout regrowth. After about 30 years, the mean number of cohorts per patch decreases significantly, leaving only a few cohorts to shape the stand's structure (Fig. 4a, inset graph). While LPD initially follows a similar trend to LPJ, disturbances that reset patches cause the cohort numbers to stabilise, and stem diameter growth levels off at a lower value than in LPJ. This stabilisation is a result of patches frequently resetting to bare ground, effectively resetting the patch age to zero. In contrast, both PPL and SEC begin with a higher density of smaller-diameter trees, because forest floor light conditions remain favourable for establishment longer than in LPJ and LPD. As a result, both models exhibit a clear decline in tree numbers due to self-thinning as stem diameter increases during the regrowth phase. Once the stand reaches around 1100 (650) trees with a mean stem diameter of approximately 18 (22) cm, the SEC (PPL) structure stabilises due to self-thinning and mortality factors linked to competition, which also create space for new trees to establish.

When comparing mortality fluxes and rates during the regrowth phase for LPJ and SEC (Fig. 5), both models display similar patterns. A strong peak in competition-based mortality occurs early in the regrowth phase due to self-thinning. As the stand ages and approaches equilibrium, the dominant mortality mechanism shifts to age- and size-related competition (Fig. 5). The increasing competition from uneven-size cohorts leads to higher mortality, as the growth efficiency of individual trees decreases due to shading from larger cohorts. During the equilibrium phase, LPJ has the fewest trees on average (N = 600), but with the largest mean DBH (Dg = 20 cm). LPD and PPL reach similar equilibrium states, with tree densities of N = 900 and N = 1200, and corresponding DBH values of Dg = 15.5 cm and 16.5 cm, respectively. SEC exhibits the highest tree density (N = 1600) but the smallest DBH (14 cm).

Analysing the Reineke self-thinning slopes (c_1) across all sites (Fig. 4) for the different canopy schemes reveals that PPL has the steepest overall slope (Table 3) during regrowth, meaning its mean DBH increases the least as tree density decreases. In contrast, SEC has the shallowest slope, resulting in the greatest increase in mean DBH during the regrowth phase. SEC, LPD, and LPJ show significant variation across temperature regions, whereas PPL does not. Tropical sites generally exhibit the steepest slopes, except for PPL, which has the shallowest slope in this region. In temperate zones, LPJ and SEC show similar slopes, while LPD has the shallowest slope. In boreal regions, SEC displays the shallowest self-thinning slope, leading

https://doi.org/10.5194/egusphere-2025-2995
Preprint. Discussion started: 4 July 2025
© Author(s) 2025. CC BY 4.0 License.

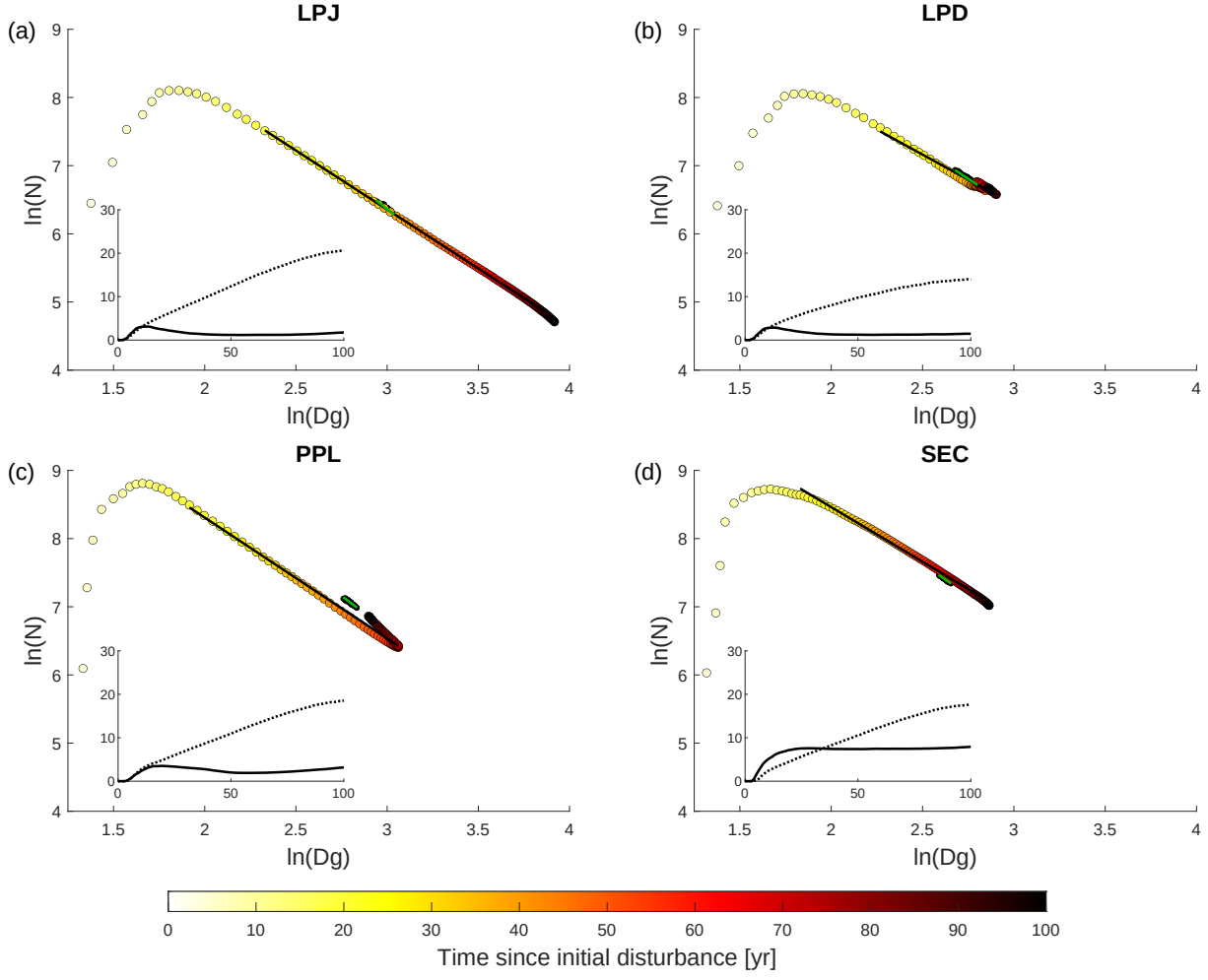

Figure 4. Tree size and density dynamics during stand regrowth (years 0 to 100) and equilibrium (years 600 to 1000) phases. N (ha^{-1}) represents the average number of trees across all sites, while Dg (cm) is the average quadratic mean diameter. The marker fill colours indicate the time elapsed since the initial disturbance that initiated the regrowth phase. Lines (black - regrowth years 20 to 90, green - equilibrium phase) represent the Reineke slope (c_1), while the black dots represent data from the equilibrium phase. The inset graph shows on the y-axis the average number of cohorts per patch (solid line) and AGB (dotted line; $\mathrm{kgC\,m}^{-2}$) across all sites during the regrowth phase years (x-axis).

to the fastest mean DBH increase as tree density decreases. Overall, the equilibrium phase tends to have a steeper slope than the regrowth phase as tree density fluctuates. PPL has the steepest slope, with SEC showing the second steepest. LPJ has the shallowest slope, particularly in the boreal region.

https://doi.org/10.5194/egusphere-2025-2995
Preprint. Discussion started: 4 July 2025
© Author(s) 2025. CC BY 4.0 License.

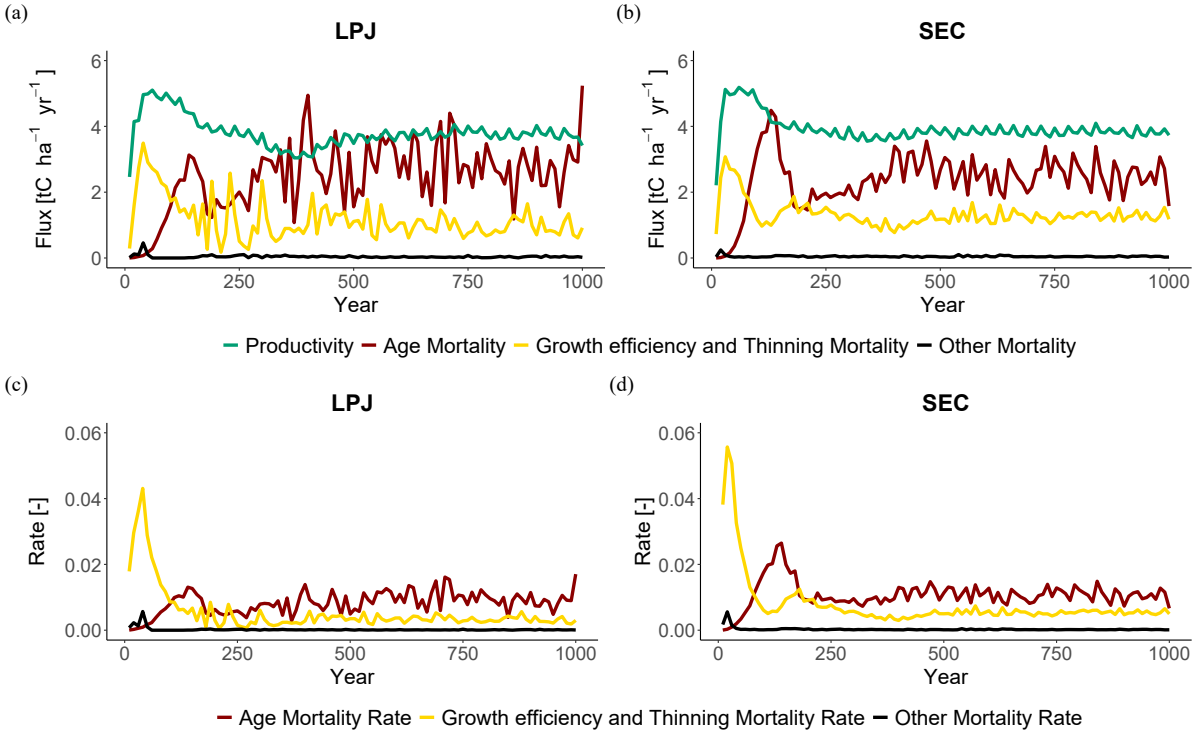

Figure 5. Mortality fluxes (top) and rates (bottom) at BCI.

Table 3. Average Reineke (1933) slope (c_1) for the regrowth (Regrow - years 20 to 90) and equilibrium (Equil - years 600 to 1000) phases across all sites and within specific temperature regions.

	LPJ		LPD		PPL		SEC	
Study sites	Regrow	Equil	Regrow	Equil	Regrow	Equil	Regrow	Equil
ALL	-1.73	-1.84	-1.62	-1.87	-1.94	-2.06	-1.61	-1.94
Boreal	-1.72	-1.56	-1.59	-1.85	-1.95	-2.12	-1.27	-1.78
Temp	-1.60	-1.84	-1.46	-1.82	-1.97	-2.10	-1.69	-1.85
Trop	-1.79	-1.92	-1.69	-1.89	-1.92	-2.02	-1.67	-2.02

3.2 Functional co-existence

LPJ simulates initial co-existence of PFTs following the patch-destroying disturbance event. However, after approximately 150 years, shade-tolerant PFTs begin to outcompete shade-intolerant PFTs, ultimately dominating the stands within 200 to 350 years (Fig. 6a). During this period, the biomass of shade-intolerant PFTs decreases to zero, while shade-tolerant PFTs maintain relatively stable biomass levels for the remainder of the simulation. LPD produces divergent results (Fig. 6b). Shade-intolerant PFTs maintain a stable biomass throughout the simulation, while shade-tolerant PFTs still dominate the ecosystem

https://doi.org/10.5194/egusphere-2025-2995
Preprint. Discussion started: 4 July 2025
© Author(s) 2025. CC BY 4.0 License.

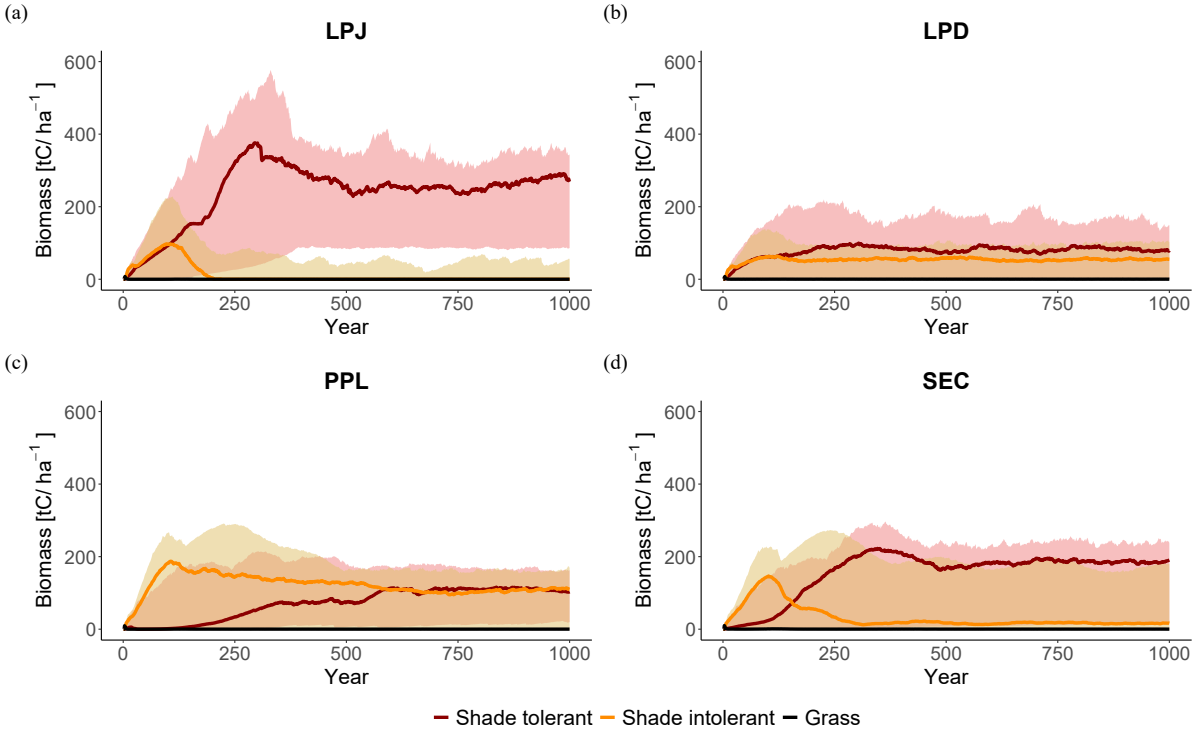

Figure 6. Comparisons of functional co-existence as an average over all study sites differentiated in shade-tolerant, shade-intolerant tree PFTs, and grasses.

on average across all sites. This dominance is more pronounced in productive areas, particularly in tropical sites, whereas in boreal regions, shade-tolerant dominance is less significant (not shown). PPL and SEC show a much higher initial biomass peak for shade-intolerant PFTs compared to LPJ and LPD (Fig. 6c and d). In PPL, shade-intolerant PFTs dominate initially, but over time, shade-tolerant PFTs co-exist at high levels, similar to the pattern seen in LPD. In contrast, shade-tolerant PFTs dominate over time in SEC, with the average biomass of shade-intolerant PFTs resembling that of LPJ. In contrast, shade-tolerant PFTs increasingly dominate over time in SEC, with the average biomass of shade-intolerant PFTs resembling that observed in LPJ. However, there is greater variability across individual sites, and some exhibiting high levels of co-existence between shade-tolerant and shade-intolerant PFTs.

All schemes initially display a typical pattern of forest dynamics: shade-intolerant PFTs establish first following a disturbance event, and over time, they are gradually replaced by shade-tolerant PFTs. LPD and PPL maintain high co-existence between these PFTs over time, whereas LPJ and SEC show less co-existence on average. When analysing the sensitivity of co-existence to changes in wood density, establishment, and mortality (Fig. 7), LPJ initially shows a strong response to doubling the wood density of shade-tolerant PFTs. Despite this, shade-tolerant PFTs eventually dominate. Changes to establishment and mortality have minimal effects on LPJ's co-existence patterns as well as little impact of establishment rates on LPD and

https://doi.org/10.5194/egusphere-2025-2995
Preprint. Discussion started: 4 July 2025
© Author(s) 2025. CC BY 4.0 License.

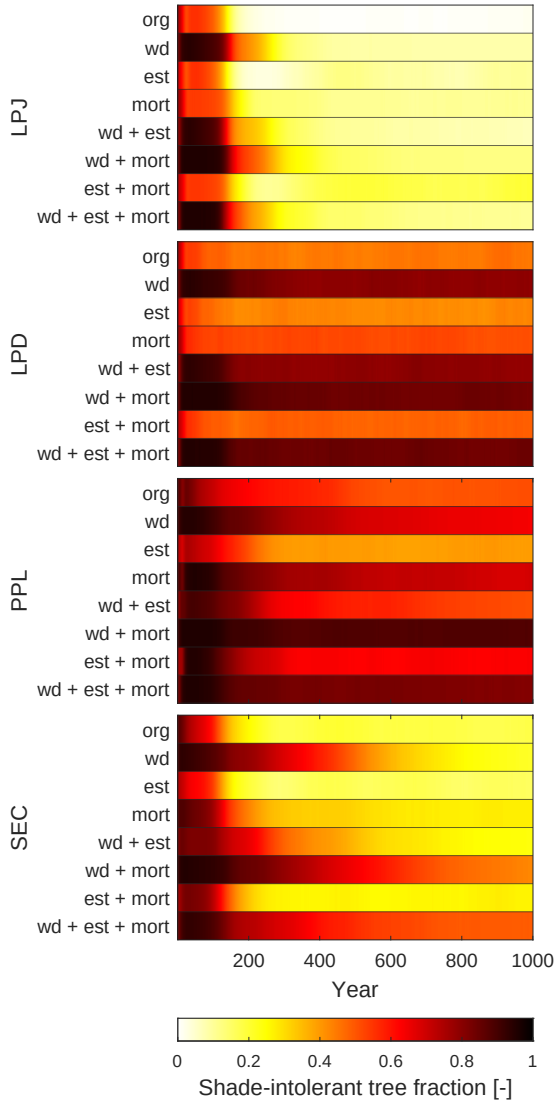

Figure 7. Fraction of co-existing shade-tolerant and intolerant PFTs when wood density (wd), establishment rate (est), and mortality rate (mort) have been changed. org - default implementation.

PPL, which already exhibit co-existence. However, alterations to wood density and mortality cause shade-intolerant PFTs to dominate, particularly with changes in wood density. For the SEC scheme, increasing wood density alone promotes higher co-existence initially, but shade-tolerant PFTs still dominate over time. When increased wood density is combined with adjustments to mortality and establishment, SEC is capable of simulating sustained co-existence throughout the simulation (Fig. 7, bottom row).

https://doi.org/10.5194/egusphere-2025-2995
Preprint. Discussion started: 4 July 2025
© Author(s) 2025. CC BY 4.0 License.

3.3 Re-establishment

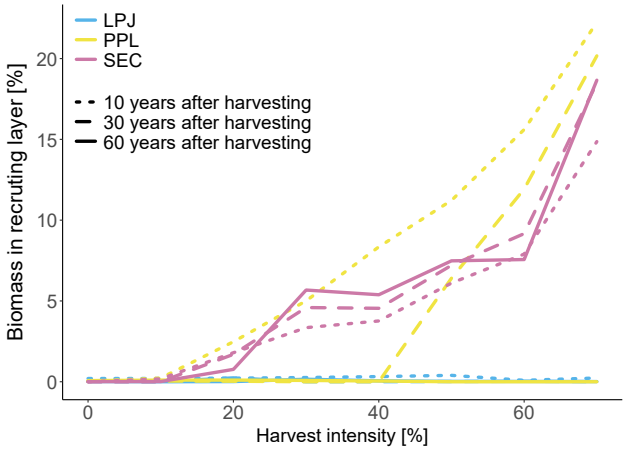

Figure 8. Re-establishment 10, 30 and 60 years after a harvest event, with a harvest strength of 0-70% at BCI. Biomass in the recruiting layer is shown as fraction of total biomass.

LPJ is unable to simulate a persistent recruitment layer at any level of harvesting at BCI (Fig. 8). In contrast, PPL can simulate the formation of a recruitment layer at a 20% harvest level, though for it to persist beyond 10 years, harvest levels above 40% are required. No harvest level allows the recruitment layer to endure for 60 years. SEC, successfully maintains a recruitment layer beyond 60 years even at a 20% harvest level, with higher harvest levels resulting in an increased fraction of stand biomass allocated to the recruitment layer.

3.4 Influence of number of patches

LPJ exhibits the highest RMSE value across all number of simulated patches when it comes to biomass, productivity, and mortality (Fig. 9). However, like PPL and SEC, it converges quickly for biomass and productivity with a relative few patches. To achieve an RMSE within 50% of the final biomass observed at 100 patches, LPJ and SEC only require 10 patches, whereas PPL needs 15 and LPD 20 patches (Fig. A4a). For productivity, LPJ, PPL, and SEC require 15 patches and LPD 20. In terms of mortality, LPJ and PPL converge more slowly than LPD and SEC, with SEC and LPD reaching convergence the fastest falling below the 50% RMSE threshold with 20 patches, while LPJ and PPL require 30 patches. Considering the different convergence rates of the canopy structure schemes, it is also important to evaluate their run times for the simulated sites in this study. Since LPD is the standard scheme in LPJ-GUESS, the different run times will be compared against it. On average, LPJ requires 1.14 times the runtime of LPD, PPL requires 1.54 times, and SEC requires 2.26 times.

https://doi.org/10.5194/egusphere-2025-2995
Preprint. Discussion started: 4 July 2025
© Author(s) 2025. CC BY 4.0 License.

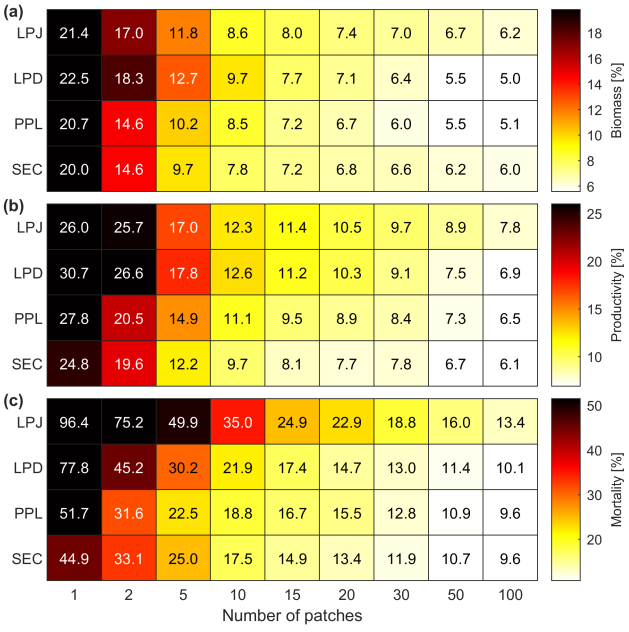

Figure 9. The impact of varying simulated patch numbers on RMSE for woody biomass (a), productivity (b), and mortality (c) against observations across all sites, excluding BCI and Finland. AGB, AWM, and AWP are normalised across DBH classes.

4 Discussion

The key reasons for incorporating the more detailed stand structure capability SEC into LPJ-GUESS were: (a) to enable closer alignment with observational data, thereby providing better constraints on the processes governing growth and mortality, and (b) to enhance the model's capability to represent critical forest features, including functional co-existence and the impacts of small-scale disturbances, such as mortality or self-thinning, on stand dynamics. In this respect, the development has been largely successful.

Simulating stand biomass-size distributions with the more detailed canopy structure schemes revealed an improvement compared to LPJ, but no improvement compared to LPD. This outcome was expected, as LPJ-GUESS has been calibrated and developed over decades using LPD. Size distributions are fundamental relationships that have shaped the model's evolution over the years. They are heavily influenced by growth and mortality rates throughout stand development and can also be significantly affected by individual disturbance events. The absence of horizontal spatial structures within a patch are favouring the dominance of the tallest tree cohort as well as the lack of patch-destroying disturbances that would otherwise reset the patch to bare ground. For LPJ this leads to an extreme shift of AWB and AWP towards larger size classes, resulting in an imprecise representation of reality. LPD as well as the new canopy schemes are able to counteract this using different approaches. LPD has been developed counting on the resetting of the patch in order to achieve a good size distribution. Figures 4, 6, and 7 clearly illustrate that the resetting of patches, caused by patch-destroying disturbances with a mean return interval of 100 years, causes

https://doi.org/10.5194/egusphere-2025-2995
Preprint. Discussion started: 4 July 2025
© Author(s) 2025. CC BY 4.0 License.

LPD to closely resemble an average state of LPJ around a stand age of 100 years. In contrast, both PPL and SEC can achieve a size distribution closer to observations without relying on patch-destroying disturbances. PPL accomplishes this by accounting for each cohort's crown area when distributing light interception between cohorts, a factor which allows more cohorts to occupy the upper canopy; the effect which is absent in LPJ and LPD. However, when the total crown area exceeds the patch area, no canopy gaps are available to support the establishment of smaller, shade-intolerant PFT cohorts. In contrast, SEC represents a mixture of size classes and allows for the formation of canopy gaps independent of the total amount of crown area, promoting the establishment of various PFTs. As light acts as a critical resource for photosynthesis, and its availability often limits plant growth in lower layers of forest ecosystems, gap formation can significantly boost photosynthetic activity, especially in newly established plants (Chazdon et al., 1996), resulting in a more accurate representation of size distributions.

Still, a need to parameterise LPJ-GUESS regarding the new canopy structure schemes is necessary to further enhance the model's ability to align with observational data. This is especially important for the representation of woody growth and woody mortality rates, which influence AGB. Here a slight shift towards larger size classes, similar to LPJ, is still present for PPL and SEC schemes. Crucially, however, the general agreement between observations and model was not degraded using the new canopy structure schemes, demonstrating that the more detailed structure was not leading to a fundamental misrepresentation of the size distribution of the forest. Supporting this, all schemes produced Reineke slope values within the ranges reported in the literature: Pretzsch and Biber (2005) reports a range from -1.42 to -1.79, and Trifković et al. (2023) from -1.19 to -2.00. Notably, the mean Reineke slope for the SEC scheme was -1.61, which closely matches the original global estimate by Reineke (1933) of -1.605.

Beyond stand biomass-size distributions, species co-existence also plays a crucial role in VDMs, which achieves a more realistic representation in the new canopy schemes. Natural disturbances create openings in the forest canopy, allowing light to reach the forest floor and give opportunities for various species to establish and co-exist, enhancing species diversity (Viljur et al., 2022). Following a gap creating disturbance, fast-growing, light-demanding species initially colonise the area. Over time, these species are replaced by slower-growing, shade-tolerant species as the canopy closes and light availability decreases (Wright et al., 2010). While shade-tolerant species with survival-focused traits tend to dominate in stable, low-light environments, shade-intolerant species grow quickly, are more prone to death and can be found in canopy gaps or disturbed areas where light is abundant (Wright et al., 2010). In order to represent species co-existence a VDM should be able to capture these dynamic processes. Also, it should be able to account for both the initial colonisation by light-demanding species and the subsequent succession to shade-tolerant species, reflecting the ecological balance driven by disturbances and canopy dynamics. Initially, LPJ demonstrates a good representation of functional co-existence (Fig. 6a and 7), however after around 200 years, even when three key growth and survival parameters are adjusted to favour shade-intolerant PFTs (Fig. 7), shade-tolerant PFTs begin to dominate, leading to the near disappearance of shade-intolerant PFTs. A higher reproduction C flux from the more abundant shade-tolerant PFTs even reinforces this dominance, further securing their strength in the ecosystem caused by a higher establishment rate. As this dominance persists even when adjusting parameters and forest structure conditions more favourable for shade-intolerant species, we conclude that a long-term co-existence with shade-tolerant species is not possible in an LPJ approach. Again, the core issue lies in this version's lack of horizontal spatial structure within the canopy. As a result, all

https://doi.org/10.5194/egusphere-2025-2995
Preprint. Discussion started: 4 July 2025
© Author(s) 2025. CC BY 4.0 License.

cohorts end up shading one another, creating an environment where shade-tolerant PFTs thrive while shade-intolerant species are disadvantaged as soon as their canopy intersects with others. This structural limitation leads to the competitive exclusion of shade-intolerant PFTs. LPD maintains a functional co-existence throughout the simulation (Fig. 6b and 7), however, these reliable results depend on the recurring patch-destroying disturbances, which reduce the average patch age of LPD to about 100 years, maintaining conditions similar to the LPJ state at year 100. As a result, the standard representation of canopy structure in LPJ-GUESS can model co-existence in young, disturbed ecosystems but will struggle to represent co-existence in old-growth, undisturbed forests, where disturbances are absent.

The new canopy schemes generate reliable results resulting from a more realistic representation of forest horizontal structure. PPL's forest composition is characterised by a high proportion of shade-intolerant PFTs (Fig. 6c, and 7), as the tallest trees are rarely shaded unless a second canopy layer forms, which occurs when the total crown area exceeds the patch area. In this case, the upper canopy is partially shaded by the second layer if the tree heights surpass the bole height of the upper-layer trees. Since shade-intolerant PFTs grow taller more rapidly than shade-tolerant PFTs, they consistently occupy the upper canopy layer with minimal disturbance. Similar to LPJ, this dominance is reinforced by the higher reproduction C flux for establishment by the dominant PFTs. The implementation of the new SEC canopy structure scheme led to a more nuanced co-existence through varying light conditions throughout the patch (Fig. 6d, and 7). We demonstrate that, in the absence of patch-destroying disturbance, an increased functional co-existence is structurally possible by only modifying three key parameters (Fig. 7). The SEC scheme permits for openings in the forest canopy, allowing light to reach the forest floor, and giving opportunities for various PFTs to establish and co-exist. This capability of representing forest gaps enhances LPJ-GUESS's capability to better represent species diversity. Following a gap-creating event, fast-growing, shade-intolerant PFTs can initially colonise the area. Over time, these PFTs are replaced by slower-growing, shade-tolerant PFTs as the canopy closes and light availability decreases. As evident in Fig. 7, the SEC canopy scheme has the capability to be parametrised to have increased or decreased co-existence.

The improvement of LPJ-GUESS by implementing more realistic canopy structure representations allows the new schemes to display a more realistic establishment after harvesting. Previous empirical studies proved the necessity of harvesting in order to promote establishment. For example, tropical forest gaps as small as 50 m^2 are shown to significantly affect species composition, while larger gaps of 100-300 m^2 are shown to actively promote new establishment of a broader range of species (Denslow, 1987). Generally, tropical forests seem to benefit from gaps ranging from 100-400 m^2, created by removing around 10-20% of canopy trees (Ghazoul et al., 2015). In mixed-species temperate forest a successful regeneration is found applying harvesting practices of removing 15-35% of live trees, simulating natural disturbances (Puettmann et al., 2012). Temperate forests are found to benefit from smaller gaps compared to tropical forests ranging from 10-150 m^2, created by removing around 15-30% of canopy trees (Larson and Churchill, 2012). For boreal forests, reducing the canopy density by 20-50%, with gaps typically ranging from 50 to 200 m^2 was found to generate sufficient light conditions, that promote the establishment of shade-intolerant species (Thorpe and Thomas, 2007). With the standard LPJ-GUESS canopy structure (LPJ), the absence of horizontal spatial structure within the canopy prevents the formation of a recruitment layer (Fig. 8). For a new cohort of any PFT to establish the average LAI must be low enough to create favourable light conditions on the forest floor. But even a 70%

https://doi.org/10.5194/egusphere-2025-2995
Preprint. Discussion started: 4 July 2025
© Author(s) 2025. CC BY 4.0 License.

reduction in LAI appears insufficient (Fig. 8). In contrast, both PPL and SEC canopy schemes generate a recruitment layer with harvest intensities as low as 20%, aligning more closely with the studies discussed earlier. Within 10 years of harvesting, PPL shows the fastest-growing recruitment layer (dash-dotted lines, Fig. 8). However, over time, PPL cannot sustain this recruitment layer. After 30 years, a harvest rate of 50% is required to maintain it, and by year 60, no recruitment layer remains. As tree crown area starts to fill the patch area in PPL, the recruitment layer is eventually shaded out once the initial cohorts have grown so that their combined crown area matches the patch area again. At the BCI site, this occurs with harvest intensities below 50% within 30 years, and by 60 years the recruitment layer disappears. In SEC, while the recruitment layer develops more slowly compared to PPL, it remains stable over time. As the canopy gaps have distinct locations, the initial cohorts must grow large enough to fill these gaps before the recruitment layer can reach sufficient height to compete for light. The proportion of biomass in the recruitment layer remains relatively constant over time for all harvest intensities that allow a recruitment layer to be established. This stability is due to the prolonged existence of the canopy gaps, which enable the recruitment layer to grow and compete with the established cohorts.

Finally, the new canopy schemes do not degrade the technical performance. To capture the distribution within a landscape, LPJ-GUESS simulates a suite of patches to represent vegetation stands with different disturbance histories and developmental stages (Smith et al., 2001, 2014). The number of patches required for LPD varies depending on the research question. For studies focused on average global fluxes and pools, approximately 15 patches may suffice. However, for questions that target site- to regional-scale dynamics, a larger number of patches is necessary to account for the variability caused by the recurring, patch-destroying disturbances. As visible in Fig. 9, LPD requires a substantial number of patches to achieve convergence when calculating the RMSE for biomass, productivity, and mortality. When the RMSE has converged, the addition of more patches will not improve the simulated result. Increased model complexity often leads to longer run times. The SEC scheme, which represents a canopy structure with greater complexity than LPD, demands more than twice the computational resources. Fortunately, SEC exhibits a faster convergence in RMSE with fewer patches, making it feasible to operate with a reduced number of patches. This capability allows for reliable results while decreasing model run duration and lowering memory usage.

5 Conclusions and outlook

The development of the new canopy structure scheme, SEC, marks a significant advancement in the representation of forest patch horizontal heterogeneity within LPJ-GUESS. This innovative scheme is capable of properly representing the size structure of biomass, productivity, and mortality across a set of sites in boreal, temperate, and tropical regions. It also allows for the representation of functional co-existence without the influence of large-scale disturbances and captures the interplay of forest gap dynamics with the establishment of a recruitment layer, an aspect which, using the standard canopy structure representation in LPJ-GUESS, was previously not possible. It is also anticipated that incorporating this more sophisticated canopy structure scheme will reduce biases related to stand structure and composition by more accurately representing the key processes driving vegetation and ecosystem dynamics. The presented results give confidence that the SEC canopy scheme can

https://doi.org/10.5194/egusphere-2025-2995
Preprint. Discussion started: 4 July 2025
© Author(s) 2025. CC BY 4.0 License.

enhance LPJ-GUESS's capability to simulate more faithfully forest demography, especially after proper parametrisation. This advancement opens up new possibilities for improving the capability of simulating various processes, such as fire and tree mortality, in a more sophisticated manner. Ultimately, this will lead to an advanced estimation of the demographic processes that drive temporal shifts in plant populations, community composition, carbon, nutrient, and water fluxes, as well as overall structure within terrestrial ecosystems, which are key processes for understanding the influence of a changing climate on our ecosystems.

Appendix A

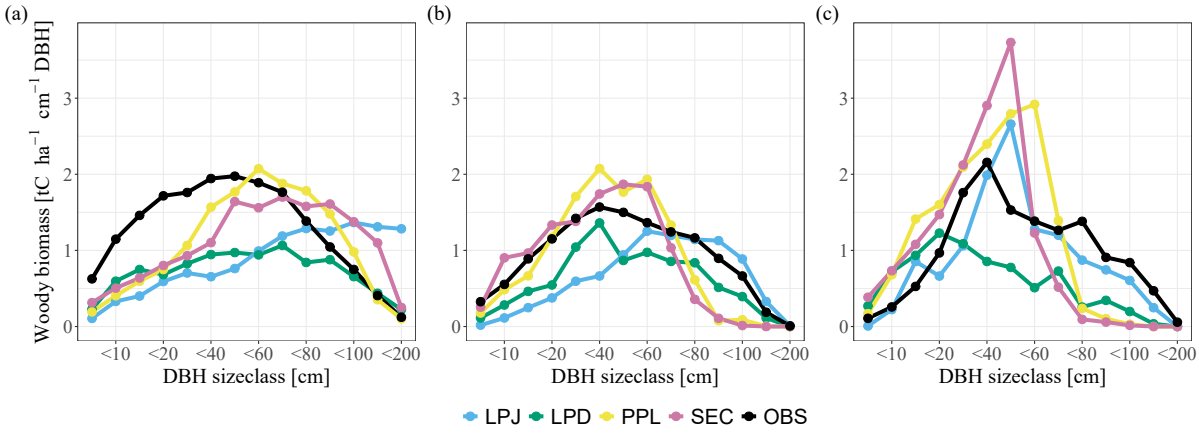

Figure A1. Comparisons of biomass as a function of DBH size class separated in the average of the (a) tropical, (b) temperate and (c) boreal sites.

https://doi.org/10.5194/egusphere-2025-2995
Preprint. Discussion started: 4 July 2025
© Author(s) 2025. CC BY 4.0 License.

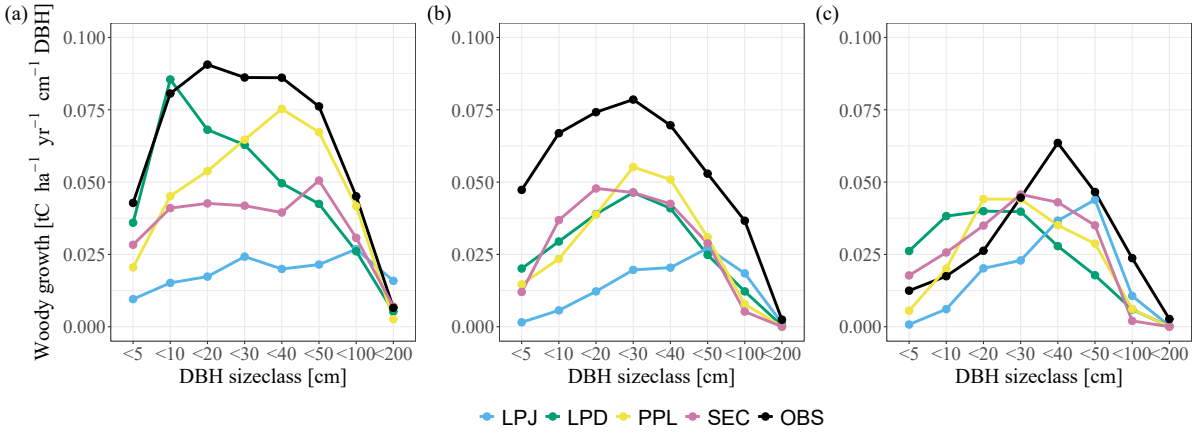

Figure A2. Comparisons of aboveground woody productivity as a function of DBH size class separated in the average of the (a) tropical, (b) temperate and (c) boreal sites.

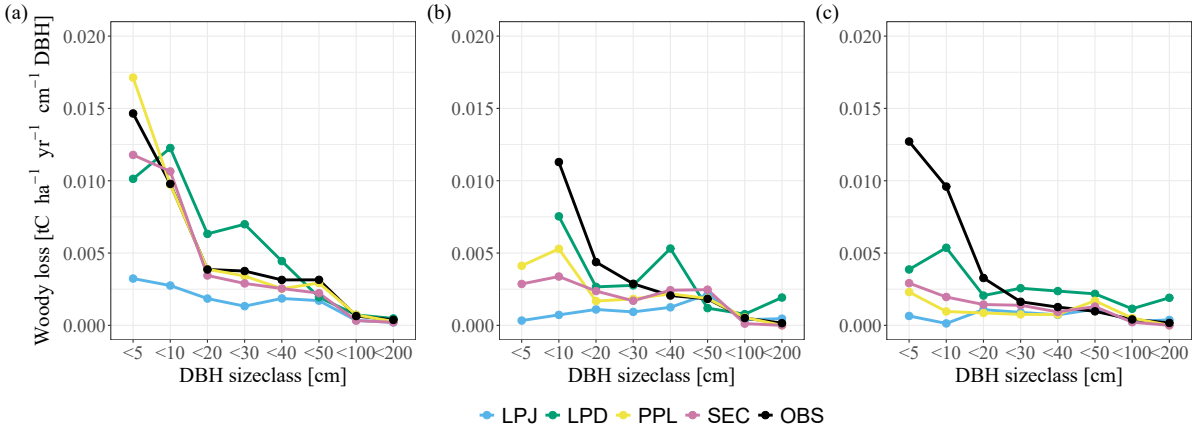

Figure A3. Comparisons of aboveground woody mortality as a function of DBH size class separated in the average of the (a) tropical, (b) temperate, and (c) boreal sites.

https://doi.org/10.5194/egusphere-2025-2995
Preprint. Discussion started: 4 July 2025
© Author(s) 2025. CC BY 4.0 License.

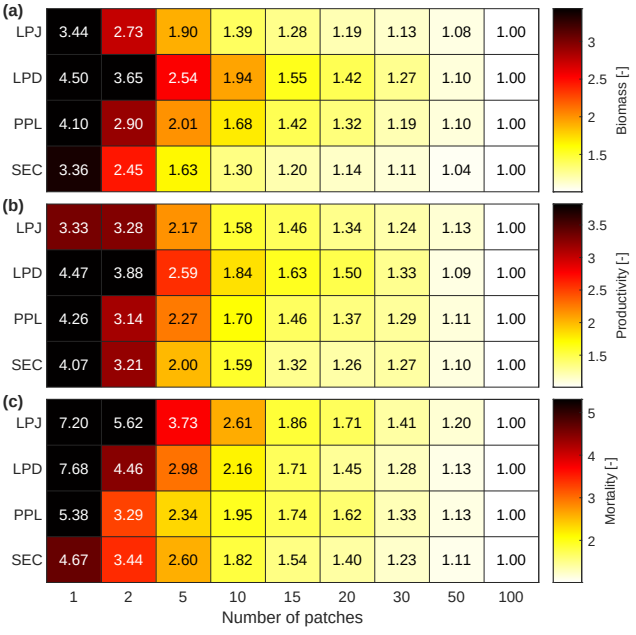

Figure A4. The influence of the number of simulated patches on RMSE value for woody biomass (a), productivity (b), and mortality (c) against observations across all study sites, excluding BCI and Finland. Same as Fig. 9, but here divided by RMSE value for 100 patches.

https://doi.org/10.5194/egusphere-2025-2995
Preprint. Discussion started: 4 July 2025
© Author(s) 2025. CC BY 4.0 License.

Code availability. The version of the LPJ-GUESS model used in this study is archived on Zenodo (https://doi.org/10.5281/zenodo.15727505; Wårlind et al. (2025)) under the Mozilla Public License 2.0.

Author contributions. DW, SO, and TAMP designed the research. DW implemented the research. JES and DW performed model simulations and data analysis. AE-S, BB, and MP contributed with data. All co-authors contributed to the data interpretation. JES prepared the manuscript with contributions from all co-authors.

Competing interests. The contact author has declared that none of the authors has any competing interests.

Acknowledgements. JS acknowledges financial support from the DAAD (German Academic Exchange Service) under the PERICLES-Project. DW acknowledges financial support from the Strategic Research Area MERGE (Modeling the Regional and Global Earth System - www.merge.lu.se) and the European Union's Horizon Europe research and innovation programme under OptimESM (grant agreement number 101081193) and GreenFeedBack (grant number 101056921). TP, SO, and AES have been funded under the European Union's Horizon 2020 programme (grant agreement number 758873, TreeMort) and the Horizon Europe research and innovation programme (grant agreement numbers 101056755, ForestPaths, and 101059888, CLIMB-Forest), as well as from the ForestValue programme, the European Commission, Vinnova, the Swedish Energy Agency and Formas for the project FORECO. MP was funded under the European Union's Horizon 2020 programme (grant agreement number 101056755, ForestPaths). This study is a contribution to the Swedish government's strategic research areas BECC and MERGE and the Nature-based Future Solutions profile area at Lund University.

https://doi.org/10.5194/egusphere-2025-2995
Preprint. Discussion started: 4 July 2025
© Author(s) 2025. CC BY 4.0 License.

References

N. S. Alwis, P. Perera, and N. P. Dayawansa. Response of tropical avifauna to visitor recreational disturbances: a case study from the sinharaja world heritage forest, sri lanka. *Avian Research*, 7(1):1–13, 2016.

V. Bellassen, G. Le Maire, J.F. Dhôte, and N Viovy. Modelling forest management within a global vegetation model - part 1: Model structure and general behaviour. *Ecol. Modelling*, 221:2458–2474, 2010. https://doi.org/10.1016/j.ecolmodel.2010.07.008.

E. G. Brockerhoff, L. Barbaro, B. Castagneyrol, D. I. Forrester, B. Gardiner, J. R. González-Olabarria, P. O'B. Lyver, N. Meurisse, A. Oxbrough, H. Taki, I. D. Thompson, F. van der Plas, and H. Jactel. Forest biodiversity, ecosystem functioning and the provision of ecosystem services. *Biodiversity and Conservation*, 26:3005–3035, 2017. https://doi.org/https://doi.org/10.1007/s10531-017-1453-2.

N. Brokaw and R. T. Busing. Niche versus chance and tree diversity in forest gaps. *Trends in ecology & evolution*, 15(5):183–188, 2000.

B. Brzeziecki, A. Pommerening, S. Miścicki, S. Drozdowski, and H. Żybura. A common lack of demographic equilibrium among tree species in białowieża national park (ne poland): evidence from long-term plots. *Journal of Vegetation Science*, 27(3):460–469, 2016.

B. Brzeziecki, K. Woods, L. Bolibok, J. Zajączkowski, S. Drozdowski, K. Bielak, and H. Żybura. Over 80 years without major disturbance, late-successional białowieża woodlands exhibit complex dynamism, with coherent compositional shifts towards true old-growth conditions. *Journal of Ecology*, 108(3):1138–1154, 2020.

R. L. Chazdon, R. W. Pearcy, D. W. Lee, and N. Fetcher. Photosynthetic responses of tropical forest plants to contrasting light environments. In *Tropical forest plant ecophysiology*, pages 5–55. Springer, 1996.

J. S. Denslow. Tropical rainforest gaps and tree species diversity. *Annual review of ecology and systematics*, pages 431–451, 1987.

M. C. Dietze, A. Fox, L. M. Beck-Johnson, J. L. Betancourt, M. B. Hooten, C. S. Jarnevich, T. H. Keitt, M. A. Kenney, C. M. Laney, L. G. Larsen, et al. Iterative near-term ecological forecasting: Needs, opportunities, and challenges. *Proceedings of the National Academy of Sciences*, 115(7):1424–1432, 2018.

I. Douglas and I. Douglas. The forests of the danum valley conservation area. *Water and the Rainforest in Malaysian Borneo: Hydrological Research at the Danum Valley Field Studies Center*, pages 27–46, 2022.

D. D'Onofrio, M. Baudena, G. Lasslop, L. P. Nieradzik, D. Wårlind, and J. von Hardenberg. Linking vegetation-climate-fire relationships in sub-saharan africa to key ecological processes in two dynamic global vegetation models. *Frontiers in Environmental Science*, 8:136, 2020. https://doi.org/10.3389/fenvs.2020.00136.

E. A. Egbe, G. B. Chuyong, B. A. Fonge, K. S. Namuene, et al. Forest disturbance and natural regeneration in an african rainforest at korup national park, cameroon. *International Journal of Biodiversity and Conservation*, 4(11):377–384, 2012.

R. Fisher, N. McDowell, D. Purves, P. Moorcroft, S. Sitch, P. Cox, C. Huntingford, P. Meir, and F. I. Woodward. Assessing uncertainties in a second-generation dynamic vegetation model caused by ecological scale limitations. *New Phytologist*, 187(3):666–681, 2010. https://doi.org/10.1111/j.1469-8137.2010.03340.x.

R. A. Fisher, C. D. Koven, W. R. L. Anderegg, B. O. Christoffersen, M. C. Dietze, C. E. Farrior, J. A. Holm, G. C. Hurtt, R. G. Knox, P. J. Lawrence, et al. Vegetation demographics in earth system models: A review of progress and priorities. *Global change biology*, 24(1): 35–54, 2018.

J. Ghazoul, Z. Burivalova, J. Garcia-Ulloa, and L. A. King. Conceptualizing forest degradation. *Trends in ecology & evolution*, 30(10): 622–632, 2015.

B. S. Hardiman, G. Bohrer, C. M. Gough, and P. S. Curtis. Canopy structural changes following widespread mortality of canopy dominant trees. *Forests*, 4(3):537–552, 2013.

https://doi.org/10.5194/egusphere-2025-2995
Preprint. Discussion started: 4 July 2025
© Author(s) 2025. CC BY 4.0 License.

T. Hickler, K. Vohland, J. Feehan, P. A. Miller, B. Smith, L. Costa, T. Giesecke, S. Fronzek, T. R. Carter, W. Cramer, I. Kühn, and M. T. Sykes. Projecting the future distribution of european potential natural vegetation zones with a generalized, tree species-based dynamic vegetation model. *Global Ecology and Biogeography*, 21(1):50–63, 2012. https://doi.org/10.1111/j.1466-8238.2010.00613.x.

J. A. Holm, J. R. Thompson, W. J. McShea, and N. A. Bourg. Interactive effects of chronic deer browsing and canopy gap disturbance on forest successional dynamics. *Ecosphere*, 4(11):1–23, 2013.

D. A. King. The adaptive significance of tree height. *The American Naturalist*, 135(6):809–828, 1990.

C. D. Koven, R. G. Knox, R. A. Fisher, J. Q. Chambers, B. O. Christoffersen, S. J. Davies, M. Detto, M. C. Dietze, B. Faybishenko, J. Holm, et al. Benchmarking and parameter sensitivity of physiological and vegetation dynamics using the functionally assembled terrestrial ecosystem simulator (fates) at barro colorado island, panama. *Biogeosciences*, 17(11):3017–3044, 2020.

G. Kunstler, S. Lavergne, B. Courbaud, W. Thuiller, G. Vieilledent, N. E. Zimmermann, J. Kattge, and D. A. Coomes. Competitive interactions between forest trees are driven by species' trait hierarchy, not phylogenetic or functional similarity: implications for forest community assembly. *Ecology letters*, 15(8):831–840, 2012.

A. J. Larson and D. Churchill. Tree spatial patterns in fire-frequent forests of western north america, including mechanisms of pattern formation and implications for designing fuel reduction and restoration treatments. *Forest Ecology and Management*, 267:74–92, 2012.

S. Lavorel and E. Garnier. Predicting changes in community composition and ecosystem functioning from plant traits: revisiting the holy grail. *Functional ecology*, 16(5):545–556, 2002.

P. Legendre and R. Condit. Spatial and temporal analysis of beta diversity in the barro colorado island forest dynamics plot, panama. *Forest Ecosystems*, 6(1):1–11, 2019.

T.-C. Lin, S. P. Hamburg, K.-C. Lin, L.-J. Wang, C.-T. Chang, Y.-J. Hsia, M. A. Vadeboncoeur, C. M. Mabry McMullen, and C.-P. Liu. Typhoon disturbance and forest dynamics: lessons from a northwest pacific subtropical forest. *Ecosystems*, 14:127–143, 2011.

C. A. López-Quintero, G. Straatsma, A. E. Franco-Molano, and T. Boekhout. Macrofungal diversity in colombian amazon forests varies with regions and regimes of disturbance. *Biodiversity and conservation*, 21:2221–2243, 2012.

N. G. McDowell, C. D. Allen, K. Anderson-Teixeira, B. H. Aukema, B. Bond-Lamberty, L. Chini, J. S. Clark, M. Dietze, C. Grossiord, A. Hanbury-Brown, et al. Pervasive shifts in forest dynamics in a changing world. *Science*, 368(6494):eaaz9463, 2020.

A. T. Michael and S. C. Hotchkiss. Ps 64-84: Spatial processes and tree fall disturbance affect understory plant community composition in hawaiian montane rainforests. In *The 94th ESA Annual Meeting*, 2009.

Ü. Niinemets and O. Kull. Effects of light availability and tree size on the architecture of assimilative surface in the canopy of picea abies: variation in needle morphology. *Tree physiology*, 15(5):307–315, 1995.

S. W. Pacala and D. H. Deutschman. Details that matter: the spatial distribution of individual trees maintains forest ecosystem function. *Oikos*, pages 357–365, 1995.

M. Peltoniemi and R. Mäkipää. Quantifying distance-independent tree competition for predicting norway spruce mortality in unmanaged forests. *Forest Ecology and Management*, 261(1):30–42, 2011.

H. A. Peters. Clidemia hirta invasion at the pasoh forest reserve: an unexpected plant invasion in an undisturbed tropical forest 1. *Biotropica*, 33(1):60–68, 2001.

C. Piponiot, K. J. Anderson-Teixeira, S. J. Davies, D. Allen, N. A. Bourg, D. F. R. P. Burslem, D. Cárdenas, C.-H. Chang-Yang, G. Chuyong, S. Cordell, et al. Distribution of biomass dynamics in relation to tree size in forests across the world. *New Phytologist*, 234(5):1664–1677, 2022.

M. D. Potts. Drought in a bornean everwet rain forest. *Journal of Ecology*, 91(3):467–474, 2003.

https://doi.org/10.5194/egusphere-2025-2995
Preprint. Discussion started: 4 July 2025
© Author(s) 2025. CC BY 4.0 License.

I. C. Prentice, M. Sykes, and W. Cramer. A simulation model for the transient effects of climate change on forest landscapes. *Ecological Modelling*, 65:51–70, 1993.

H. Pretzsch and P. Biber. A re-evaluation of reineke's rule and stand density index. *Forest Science*, 51:304–320, 2005. https://doi.org/https://doi.org/10.1093/forestscience/51.4.304.

K. J. Puettmann, K. D. Coates, and C. C. Messier. *A critique of silviculture: managing for complexity*. Island press, 2012.

T. A. M. Pugh, A. Arneth, M. Kautz, B. Poulter, and B. Smith. Important role of forest disturbances in the global biomass turnover and carbon sinks. *Nature Geoscience*, 12:730–735, 2019a. https://doi.org/10.1038/s41561-019-0427-2.

T. A. M. Pugh, M. Lindeskog, B. Smith, B. Poulter, A. Arneth, V. Haverd, and L. Calle. Role of forest regrowth in global carbon sink dynamics. *Proceedings of the National Academy of Sciences of the United States of America*, 116(10):4382–4387, 2019b. https://doi.org/10.1073/pnas.1810512116.

T. A. M. Pugh, M. Lindeskog, B. Smith, B. Poulter, A. Arneth, V. Haverd, and L. Calle. Role of forest regrowth in global carbon sink dynamics. *Proceedings of the National Academy of Sciences*, 116(10):4382–4387, 2019c.

T. A. M. Pugh, R. Seidl, D. Liu, M. Lindeskog, L. P. Chini, and C. Senf. The anthropogenic imprint on temperate and boreal forest demography and carbon turnover. *Global Ecology and Biogeography*, 33(1):100–115, 2024. https://doi.org/10.1111/geb.13773.

D. W. Purves, J. W. Lichstein, N. G. Strigul, and S. W. Pacala. Predicting and understanding forest dynamics using a simple tractable model. *Proceedings of the National Academy of Sciences*, 105(44):17018–17022, 2008. https://doi.org/10.1073/pnas.0807754105.

L. H. Reineke. Perfecting a stand-density index for even aged forests. *Journal of Agricultural Research*, 46:627–638, 1933.

H. Sato, A. Itoh, and T. Kohyama. Seib–dgvm: a new dynamic global vegetation model using a spatially explicit individual-based approach. *Ecological Modelling*, 200:279–307, 2007. https://doi.org/https://doi.org/10.1016/j.ecolmodel.2006.09.006.

D. C. Shaw, J. F. Franklin, K. Bible, J. Klopatek, E. Freeman, S. Greene, and G. G. Parker. Ecological setting of the wind river old-growth forest. *Ecosystems*, 7:427–439, 2004.

S. Sitch, B. Smith, I. C. Prentice, A. Arneth, A. Bondeau, W. Cramer, J. O. Kaplan, S. Levis, W. Lucht, K. Sykes, M. Thonicke, and S. Venevsky. Evaluation of ecosystem dynamics, plant geography and terrestrial carbon cycling in the lpj dynamic global vegetation model. *Global change biology*, 9(2):161–185, 2003.

S. Sitch, C. Huntingford, N. Gedney, P. E. Levy, M. Lomas, S. L. Piao, R. Betts, P. Ciais, P. Cox, P. Friedlingstein, et al. Evaluation of the terrestrial carbon cycle, future plant geography and climate-carbon cycle feedbacks using five dynamic global vegetation models (dgvms). *Global change biology*, 14(9):2015–2039, 2008.

B. Smith, I. C. Prentice, and M. T. Sykes. Representation of vegetation dynamics in the modelling of terrestrial ecosystems: comparing two contrasting approaches within european climate space. *Global ecology and biogeography*, pages 621–637, 2001. URL http://www.jstor.org/stable/3182691.

B. Smith, D. Wårlind, A. Arneth, T. Hickler, P. Leadley, J. Siltberg, and S. Zaehle. Implications of incorporating n cycling and n limitations on primary production in an individual-based dynamic vegetation model. *Biogeosciences*, 11(5):2027–2054, 2014. https://doi.org/https://doi.org/10.5194/bg-11-2027-2014.

R. Sukumar, H. S. Suresh, H. S. Dattaraja, R. John, and N. V. Joshi. Mudumalai forest dynamics plot, india, 2004.

H. C. Thorpe and S. C. Thomas. Partial harvesting in the canadian boreal: success will depend on stand dynamic responses. *The Forestry Chronicle*, 83(3):319–325, 2007.

V. Trifković, A. Bončina, and A. Ficko. Density-dependent mortality models for mono- and multi-species uneven-aged stands: The role of species mixture. *Forest Ecology and Management*, 545:121260, 2023. https://doi.org/https://doi.org/10.1016/j.foreco.2023.121260.

https://doi.org/10.5194/egusphere-2025-2995
Preprint. Discussion started: 4 July 2025
© Author(s) 2025. CC BY 4.0 License.

F. Van der Plas, S. Ratcliffe, P. Ruiz-Benito, M. Scherer-Lorenzen, K. Verheyen, C. Wirth, M. A. Zavala, E. Ampoorter, L. Baeten, L. Barbaro, et al. Continental mapping of forest ecosystem functions reveals a high but unrealised potential for forest multifunctionality. *Ecology letters*, 21(1):31–42, 2018.

M.-L. Viljur, S. R. Abella, M. Adámek, J. B. R. Alencar, N. A. Barber, B. Beudert, L. A. Burkle, L. Cagnolo, B. R. Campos, A. Chao, et al. The effect of natural disturbances on forest biodiversity: an ecological synthesis. *Biological Reviews*, 97(5):1930–1947, 2022.

J. B. Vincent, B. Henning, S. Saulei, G. Sosanika, and G. D. Weiblen. Forest carbon in lowland p apua n ew g uinea: Local variation and the importance of small trees. *Austral Ecology*, 40(2):151–159, 2015.

N. Viovy. Cruncep version 7 – atmospheric forcing data for the community land model. *Research Data Archive at the National Center for Atmospheric Research, Computational and Information Systems Laboratory*, 2016. https://doi.org/doi:10.5065/PZ8F-F017.

R. H. Waring and S. W. Running. *Forest ecosystems: analysis at multiple scales*. Elsevier, 2010.

Jamie M Waterman, Anthony W D'Amato, David R Foster, David A Orwig, and Neil Pederson. Historic forest composition and structure across an old-growth landscape in new hampshire, usa1. *The Journal of the Torrey Botanical Society*, 147(4):291–303, 2020.

S. Weng, E. S.and Malyshev, J. W. Lichstein, C. E. Farrior, R. Dybzinski, T. Zhang, E. Shevliakova, and S. W. Pacala. Scaling from individual trees to forests in an earth system modeling framework using a mathematically tractable model of height-structured competition. *Biogeosciences*, 12(9):2655–2694, 2015. https://doi.org/doi:10.5194/bg-12-2655-2015.

S. J. Wright, K. Kitajima, N. J. B. Kraft, P. B. Reich, I. J. Wright, D. E. Bunker, R. Condit, J. W. Dalling, S. J. Davies, S. Díaz, et al. Functional traits and the growth-mortality trade-off in tropical trees. *Ecology*, 91(12):3664–3674, 2010.

D. Wårlind, B. Smith, T. Hickler, and A. Arneth. Nitrogen feedbacks increase future terrestrial ecosystem carbon uptake in an individual-based dynamic vegetation model. *Biogeosciences*, 11(21):6131–6146, 2014. https://doi.org/10.5194/bg-11-6131-2014.

D. Wårlind, J. E. Stoebke, S. Olin, and T. Pugh. Representing canopy structure dynamics within the lpj-guess dynamic global vegetation model (revision 13221). *Dataset on Zenodo*, 2025. https://doi.org/10.5281/zenodo.1153887.

Y. Zhang, A. Wang, Y. Liu, L. Shen, R. Cai, and J. Wu. Disturbance of wind damage and insect outbreaks in the old-growth forest of changbai mountain, northeast china. *Forests*, 14(2):368, 2023.

J. K. Zimmerman, T. E. Wood, G. González, A. Ramirez, W. L. Silver, M. Uriarte, M. R. Willig, R. B. Waide, and A. E. Lugo. Disturbance and resilience in the luquillo experimental forest. *Biological Conservation*, 253:108891, 2021.